Journal of Theoretical and Applied Information Technology
31st July 2013. Vol. 53 No.3

ISSN: 1992-8645 www.jatit.org E-ISSN: 1817-3195

AN EVOLUTIONARY PROGRAMMING APPROACH TO OPTIMIZE SYNCHRONOUS GENERATOR INPUT POWER USING AREA-BASED TRANSIENT STABILITY INDEXES

[1]H. HASHIM, [2]I. Z. ABIDIN, [3]I. MUSIRIN, [4]KEEM SIAH YAP, [5]Y. R. OMAR, [6]M. R. ZULKEPALI
[1]Senior Lecturer, Department of Electrical Engineering, UNITEN, Malaysia
[2]Assoc. Prof., Department of Electrical Engineering, UNITEN, Malaysia
[3]Assoc. Prof., Department of Electrical Engineering, UITM, Malaysia
[4]Senior Lecturer, Department of Electrical Engineering, UNITEN, Malaysia
[5]Senior Lecturer, Department of Electrical Engineering, UNITEN, Malaysia
[6]Electrical Engineer, Tenaga Nasional Berhad, Malaysia
E-mail:[1]halimatun@uniten.edu.my, [2]izham@uniten.edu.my, [3] ismailbm@salam.uitm.edu.my, [4]Yapkeem@uniten.edu.my, [5]Yaakob@uniten.edu.my, [6]ridzuwan.zulkepali@tnb.com.my

ABSTRACT

Stable operation of a power system requires a continuous match between energy input to the prime movers and the electrical load of the system. Any change of load demand must be accompanied by a corresponding change in terms of the amount of energy prime mover given to the turbine system. When a power system is subjected to significant transient disturbances, the machine may lose synchronism to the system. If this were to happen, the machine's rotor angle will undergo wide variations, voltage and frequency may deviate widely from normal values. This paper presents the applications of Area-Based Transient Stability Indexes (TSI): COI Angle and COI Speed as a new technique to evaluate the impact of disturbances to power system stability and to optimize the mechanical input power of synchronous generators in order to prevent transient instability in a power system using Evolutionary Programming (EP) approach. Transient analysis is carried out using PSS®E software on IEEE 118 Bus Test System at system conditions with various types of loads, static and dynamic. The optimization of the input power to generator is carried out using transient stability indexes as fitness functions for a three area IEEE 30 Bus and IEEE 118 Bus Test Systems respectively. Results obtained from the experiment revealed that the EP approach is able to give an optimal solution.

Keywords: *Area-Based Transient Stability Indexes: COI Angle and COI Speed, Optimization, Evolutionary Programming*

1. INTRODUCTION

Transient stability is concerned with the ability of the power system to be in equilibrium when subjected to a severe disturbance [1]-[3] such as major fault on transmission facilities, large loss of load or generation. These types of fault may cause a large amount of kinetic energy being imposed to the power system, which will result to large flow of fault currents and variation of torque experienced by the machine concerned. When the difference between the mechanical input power to a generator, P_m and the electrical output power, P_e is significant, an unbalanced torque may act on the rotor, which causes the generator to either accelerate or decelerate. In another word, the generator's operating point may oscillate as such its oscillation may lead to out-of-step or loss of synchronism due to the large excursion of generator rotor angle [1], [3]-[6]. The system is in a state of transient instability if one or more generators fall out of step with respect to the rest of the system [7]-[8]. If the mechanical input power does not rapidly match the electrical power load demand, the turbine speed of the generator will not be at its optimal speed; hence, system parameters will be affected, frequency and voltage will deviate from their nominal values. The impact is propagated in the respective power system network.

Research carried out on transient stability can be in the form of transient stability assessment, which includes analyses on the out-of-step condition. Most of power system stability books,

ISSN: 1992-8645 www.jatit.org E-ISSN: 1817-3195

papers and journals used classical equal area criteria based on the accelerating and decelerating energies to analyze an out of step condition. However, some may monitor the variation of apparent impedance viewed at a line or generator terminals as a function of system voltages and angular separation between the systems. It is formulated during a loss of synchronism either between two system areas or between a generator and a system. Reference [7] applied a modified time domain equal area criterion technique to discriminate between stable and out-of-step swings based on the local voltage and current information available at the relay location while [8] detected an out-of-step phenomenon based on the variation of resistance, the behavior of the impedance loci.

Neural network is another method to identify the unstable out-of-step based on rotor angle excursion [9]: if the rotor angle of the generator under study reaches 180° within 1s the system is classified as unstable with a given stability index of 0, otherwise the sample is classified as stable, and it is given a stability index of 1. This method considered three factors: the pre-fault loading of the generator or the mechanical input power P_m; the generator kinetic energy deviation the instant of fault clearing; and the average acceleration during fault. An out-of-step condition can also be classified based on the three characteristics of the separation interface tie-lines [10]: first, the active power on these lines crosses zero and oscillates periodically; second, the existence of out-of-step center point on the separation interface, whose voltage fluctuation amplitude is significantly larger than that of other points; third, the reactive power flows into the interior from both sides of the separation interface. Similarly, reference [11] tracked the changing of the voltage oscillation center through synchrophasor measurements to detect the synchronism loss as an adaptive power system separation criterion.

An angular excursion of instantaneous voltage values can be translated into angular velocity and angular acceleration and used to detect an out-of-step condition [12]. A protective relay that applies this concept is more sensitive compared to distance relay, which applies impedance variation principle. Center of Inertia (COI) reference frame [3]-[5] is being widely used in transient stability analysis for various specific objective(s) and approaches including to monitor, evaluate and predict system stability, improve transient stability, optimize power flow, design a controller for STATCOM, and split the system network [2], [13]-[21]. Important parameters such as angle, speed, power are converted to COI frame to derive a first swing stability index as an additional output quantity from the time domain simulation [13]. Reference [2] uses transient stability index as a new transient stability forecast, which can predict both transient stability status and tripped units. The values of measured rotor angles in the COI coordinates values, δ_i^{COI} at fault clearing time and a few cycles after fault clearing time are considered as the input information of the forecast process. δ_i^{COI} will determine the chances of saving or losing synchronism.

For a large power system it is easier to track the system stability based on the stability of interconnected areas where generators' rotor angles in the system are being assessed based on area [13]-[14]. This reference introduced area-based Center of Inertia (COI) referred Transient Stability Index that represents a group of generators in the respective area to assess the stability of the system, focusing on the COI-referred rotor angles. The difference between this paper and reference [14] in terms of power system stability analysis is this paper evaluates the impact of disturbances in power system with different types of loads, static and dynamic loads using Area-Based: TSI COI Angle and TSI COI Speed. Nevertheless, reference [14] focused only on the COI-referred rotor angles. With TSI COI Speed included in the transient stability analysis, the evaluation becomes more firm to signify the dynamic state with the fact that a multi-machine system is in synchronism with all the machines turning at a constant speed [4]. Hence, the transient stability analysis in this paper includes the TSI COI Speed of the synchronous generators, which at the same time reflects the frequency of the system.

This paper consists of two parts: first, transient stability analysis is carried out by studying the behavior of rotor angles in each area of IEEE118 Bus Test System. The stability of this system is further examined based on the Accelerating Power and Area-Based: TSI COI Angle and TSI COI Speed. Second, an EP approach is used to optimize synchronous generator input power using area-based transient stability indexes. In this study, mechanical input power is optimized to prevent transient instability in the system that includes angular instability, frequency instability and voltage instability. The optimization is based on Area-based: TSI COI Angle and TSI COI Speed.

Journal of Theoretical and Applied Information Technology
31st July 2013. Vol. 53 No.3

ISSN: 1992-8645 www.jatit.org E-ISSN: 1817-3195

The angular and frequency stabilities are governed by two fitness functions: TSI COI Angle and TSI COI Speed respectively while voltage stability is being controlled by the constant and control variables. The algorithm is tested using three area system on two test systems: IEEE 30 Bus Test System with 6 generators and IEEE 118 Bus Test System with 28 generators.

Two optimization engines have been developed to optimize TSI COI Angle and TSI COI Speed, making them a single objective optimization implemented separately. Results obtained from the experiment revealed that the EP approach is able to give an optimal solution. The comparative studies are conducted with respect to the conclusions obtained from transient stability analysis on IEEE 118 bus test system so as to validate the acceptable numerical values for system stability analysis implemented using EP.

2. AREA-BASED: TSI COI ANGLE AND TSI COI SPEED

Synchronism assessment among generators when the system is subjected to disturbances can be made by looking into the variation of rotor angle [2]. The system is not stable if the rotor angle of a generator increases with respect to the rest of the system. Similarly, the angular velocity can be translated to system frequency. For a multi-machine system, Area-Based TSI COI Angle and TSI COI Speed are common transformation used in transient stability analysis [4] being derived based on the swing equation.

$$M\frac{d^2\delta}{dt^2} = P_m - P_e \quad (1)$$

Where M is the moment of inertia of the machine, δ is the electrical power angle, P_m is the mechanical power and P_e is the electrical power.

The indexes shown in equation (2) and equation (6) relate to the rotor angle and angular speed of a particular area of a power grid and are based on an equivalent inertia representing the total inertia of the generators located in that area. The indexes are derived from the classical machine model by assuming that the dynamic behavior of generators in the system [3]-[5]. If the indexes calculated show an out of step condition after the fault is cleared, the system is considered to be in an unstable condition. In addition, if the multi-machine system is in synchronism with all the machines turning at a constant speed, the system frequency is equal to the dynamic frequency (possibly above or below the steady state speed, ω_s) [4].

The COI reference transformation defines the COI Angle and COI Speed instead of referring to the angle of a specific machine. The COI reference transformation defines the TSI COI Angle as [14]:

$$\delta_j^{coi} = \bar{\delta}_j - \bar{\delta}_{COI} \quad (2)$$

$$\bar{\delta}_j = \frac{1}{N}\sum_{i=1}^{N} \delta_i \quad (3)$$

$$\bar{\delta}_{COI} = \frac{1}{M_T}\sum_{j=1}^{r} M_i\bar{\delta}_i \quad (4)$$

$$M_T = \sum_{i=1}^{r} M_i \quad (5)$$

Where N is the number of generator, M_T is the total system inertia, δ_i is the individual rotor angle, $\bar{\delta}_j$ is the area equivalent rotor angle of each area, $\bar{\delta}_{COI}$ is the COI Angle of the system while r is total number of areas in a power system. The COI reference transformation defines the TSI COI Speed as:

$$\omega_j^{coi} = \bar{\omega}_j - \bar{\omega}_{COI} \quad (6)$$

$$\bar{\omega}_j = \frac{1}{N}\sum_{i=1}^{N} \omega_i \quad (7)$$

$$\bar{\omega}_{COI}(t) = \frac{1}{M_T}\sum_{j=1}^{r} M_j\bar{\omega}_j \quad (8)$$

Where ω_i is the individual rotor speed, $\bar{\omega}_j$ is the area equivalent rotor speed and $\bar{\omega}_{COI}$ is the COI Speed of the system.

3. OPTIMIZATION OF MECHANICAL INPUT POWER

It is important to analyze the impact of disturbances to the power network in order to maintain system stability and to anticipate the correct amount of mechanical power when the system is subjected to large disturbances in order to minimize supply interruption and hence maintain system stability. Figure 1 shows the general EP algorithm, which is used as an approach to optimize the mechanical input power to synchronous generators in the system, taking into consideration the relevant control variables.

Journal of Theoretical and Applied Information Technology
31st July 2013. Vol. 53 No.3

ISSN: 1992-8645 www.jatit.org E-ISSN: 1817-3195

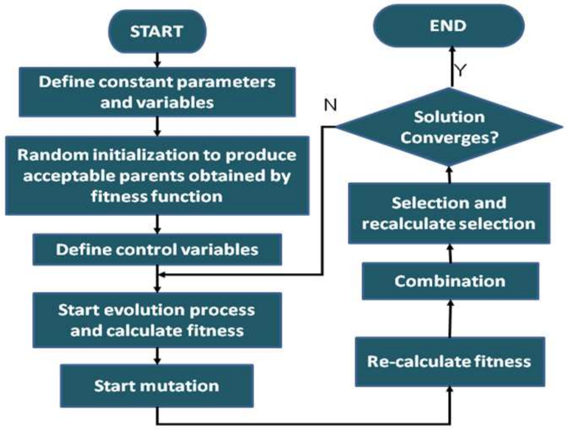

Figure 1: The EP Algorithm To Optimize The Mechanical Input Power

The problem formulation is based on the two equations derived by [1]:

$$\delta = \delta_0 + \frac{180 f_0 \Delta P}{H \omega_n^2}\left[1 - \frac{1}{(1-\zeta^2)^{0.5}} e^{-\zeta\omega_n} \sin(\omega_d t + \theta)\right] \quad (9)$$

$$\omega = \omega_0 + \frac{\pi f_0 \Delta P}{H \omega_n (1-\zeta^2)^{0.5}} e^{-\zeta\omega_n} \sin(\omega_d t + \theta) \quad (10)$$

The fitness functions are based on Area-Based TSI COI Angle and TSI COI Speed taking into consideration the fault clearance time, which depends on the system voltage [23]. The criteria for system stability are the TSI COI Angle must be within ±180º and the TSI COI Speed is within certain limit depending on the tolerance of system frequency. With these two constraints, the fitness functions for TSI COI Angle and TSI COI Speed are formulated.

4. TEST SYSTEM

Two IEEE test systems are used in this paper: IEEE 30-Bus and IEEE 118-Bus test systems. IEEE 30 bus test system as shown in Figure A1 in the Appendix consists of 6 generators in 3 Areas, 40 lines including 7 tie-lines. IEEE 118-Bus Test System consists of 28 generators, 118 buses and 186 transmission lines. Figure A2 in the Appendix shows that this large network is divided into three areas, namely: Area 1 has 13 generators, Area 2 with 8 generators and Area 3 consists of 7 generators respectively based on geographical. Different types of power plants are modeled namely: hydro, coal and gas and they are connected to static loads and/or dynamic loads using PSS®E software. The characteristic of rotor angle for each machine in the respective area with respect to randomly selected reference machine was plotted during pre-fault, fault and post-fault conditions. To evaluate the stability of the system, data obtained from the simulation results were used to calculate the stability indexes. If the TSI COI Angle is within ±180º and the TSI COI Speed is very low, the system is in stable condition; however, if the TSI COI Angle exceeds ±180º [4], [14]-[15] and the TSI COI Speed is large, then the system is in an unstable condition.

In addition, the Evolutionary Programming based on the algorithm in Fig. 1 is implemented on a 3 area system that consists of 6 generators with two generators in each area: G_1 and G_2 in Area 1, G_3 and G_4 in Area 2; G_5 and G_6 in Area 3. Results obtained from both methods are analyzed using TSI COI Angle and TSI COI Speed.

5. RESULTS AND ANALYSES

The processed results obtained from transient analysis study on the IEEE 118-Bus Test System are used to validate the acceptable numerical values for system stability analysis implemented using EP.

5.1 PSS®E Simulation on IEEE 118-Bus Test System

Findings from the two case studies of transient study analysis are presented to show the applications of TSI COI Angle and TSI COI Speed**.** Case 1 shows the scenario for generators in synchronism. A fault was applied at Bus 49 with a fault clearance time of 100ms [23]. Figure 3 to 5 illustrate the behavior of the rotor angles in each area. All the generators other than Generator 49 are in synchronism at each area. The generators' rotor angles settled at values which are lower than 90° in less than 10 seconds with small oscillation while generator 49 losses synchronism and its rotor angle infinitely increases.

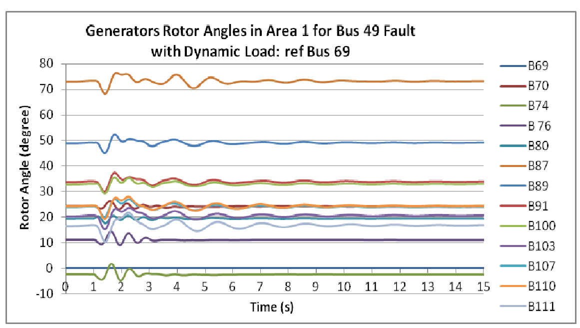

Figure 3: Generators' response in Area 1for a fault at Bus 49 in Area 2 – Case 1.

Journal of Theoretical and Applied Information Technology
31st July 2013. Vol. 53 No.3

ISSN: 1992-8645 www.jatit.org E-ISSN: 1817-3195

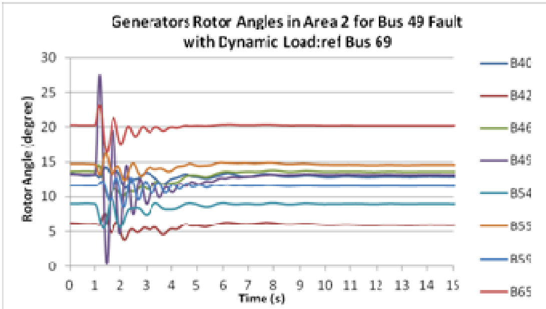

Figure 4: Generators' response in Area 2 for a fault at Bus 49 in Area 2 – Case 1.

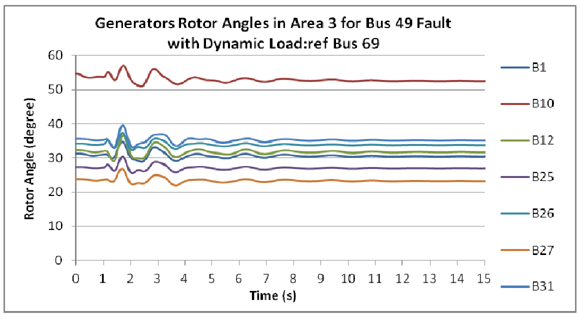

Figure 5: Generators' response in Area 3 for a fault at Bus 49 in Area 2 – Case 1.

Table 1 tabulates the TSI COI Angle and TSI COI Speed respectively calculated at 20 seconds. The TSI COI Angle at each area is lesser than ±180°, which proves the system is in stable condition and reflects that the generators in Area 1, Area 2 and Area 3 are operating in synchronism.

Table 2 demonstrates that the TSI COI Speed is very low, which implies that this multi-machine system is in synchronism with all the machines in each area turning at almost a constant speed, either slightly above or below the steady state speed, ω_s. Hence, the system frequency is almost equal to the dynamic frequency. Thus, Table 2 supports the analysis made from Table 1, which indicates that the system is stable.

Table 1: Case 1 - TSI COI Angle at t = 15s for Bus 49 Fault with Dynamic Load

Area equivalent rotor angle	$\bar{\delta}_1 = 25.242°$	$\bar{\delta}_2 = 12.623°$	$\bar{\delta}_3 = 33.362°$
System COI Angle	$\bar{\delta}_{COI}(t) = \frac{1}{M_T}\sum_{j=1}^{r} M_j\bar{\delta}_j = 23.737°$		
Area-Based TSI COI Angle	$\delta_1^{COI} = 1.505$	$\delta_2^{COI} = -11.114°$	$\delta_2^{COI} = 9.625°$

Table 2: Case 1 - TSI COI Speed at t = 15s for Bus 49 Fault with Dynamic Load

Area equivalent rotor speed (rad/s)	$\bar{\omega}_1 = 314.1590$	$\bar{\omega}_2 = 314.1595$	$\bar{\omega}_3 = 314.1611$
System COI Speed (rad/s)	$\bar{\omega}_{COI}(t) = \frac{1}{M_T}\sum_{j=1}^{r} M_j\bar{\delta}_j = 314.1597$		
Area-Based TSI COI Speed (rad/s)	$\omega_1^{COI} = -0.0007$	$\omega_2^{COI} = -0.0002$	$\omega_3^{COI} = 0.0014$

The stability of the system is further confirmed by analyzing the graphical illustrations of TSI COI Angle, TSI COI Speed and Accelerating Power for the three areas as in Figure 6 - 8: the graphs of TSI COI Angle versus time are at low values, lower than ±180°; the graphs of TSI COI Speed versus time are converging and similarly with the graph of Accelerating Power versus time.

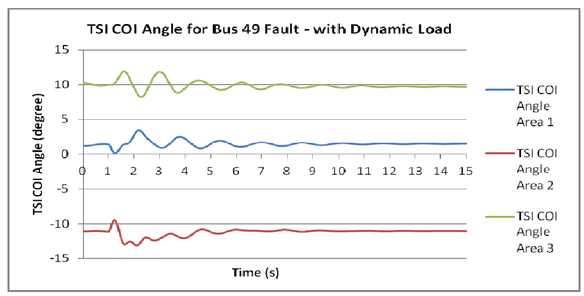

Figure 6: Plots of TSI COI Angle for Bus 49 Fault with Dynamic Load

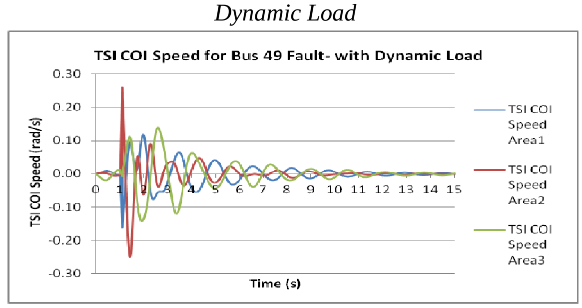

Figure 7: TSI COI Speed for Bus 49 Fault with Dynamic Load

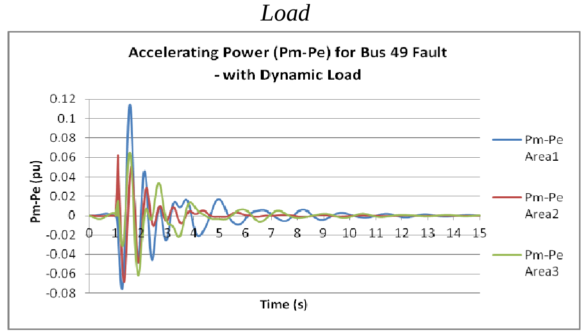

Figure 8: Accelerating Power for Bus 49 Fault with Dynamic Load

Journal of Theoretical and Applied Information Technology
31st July 2013. Vol. 53 No.3

ISSN: 1992-8645 www.jatit.org E-ISSN: 1817-3195

Case 2 exhibits the phenomena when generators are out of synchronism. Bus 80 was disconnected due to a fault occurred in the system and cleared after 100ms. Fig. 8 to 10 demonstrate the behavior of the rotor angles in each area. Most of the generators in Area 1 are out of synchronism while the rotor angle of Generator 80 increases infinitely. In contrast, all generators in Area 2 and Area 3 remain in synchronism with small signal oscillations due to the occurrence of severe fault in the system.

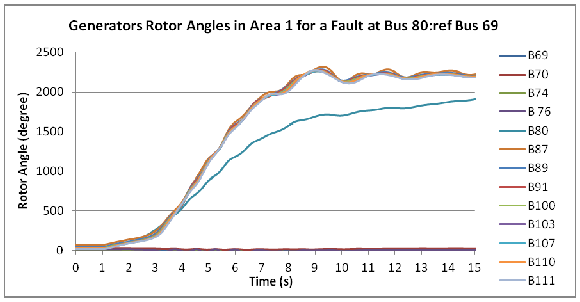

Figure 9: Generators' response in Area 1 for a fault at Bus 80 Fault with Dynamic Load - Case2.

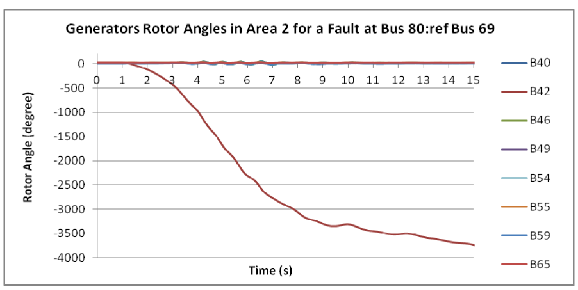

Figure 10: Generators' response in Area 2 for a fault at Bus 80 Fault with Dynamic Load – Case 2

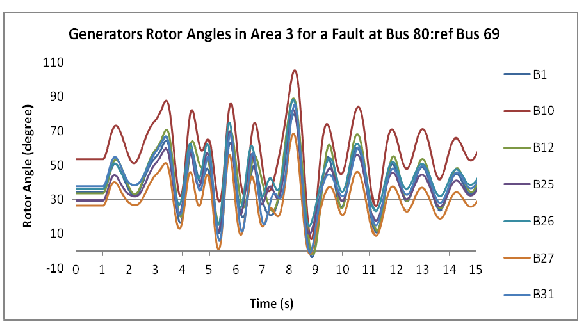

Figure 11: Generators' response in Area 3 for a fault at Bus 80 Fault with Dynamic Load – Case 2

Table 3 and Table 4 tabulate the value of Area-Based TSI: COI Angle and COI Speed respectively calculated at 15 seconds. The Area-Based TSI: COI Angle at each area is exceeding ±180°, which indicates that the system is unstable.

Table 3: Case 2 - TSI COI Angle at t = 15s for Bus 80 Fault with Dynamic Load

Area equivalent rotor angle	$\bar{\delta}_1 = 1502°$	$\bar{\delta}_2 = 451°$	$\bar{\delta}_3 = 39°$
System COI Angle	$\bar{\delta}_{COI}(t) = \frac{1}{M_T}\sum_{j=1}^{r} M_j\bar{\delta}_j = 564°$		
Area-Based TSI COI Angle	$\delta_1^{COI} = 938°$	$\delta_2^{COI} = 1015°$	$\delta_3^{COI} = -525°$

The values of Area-Based TSI: COI Speed are multiple times higher than the values in Table 2, which further emphasize that the system is in unstable condition. The system frequency is not equal to the dynamic frequency.

Table 4: Case 2 - TSI COI Speed at t = 15s for Bus 80 Fault with Dynamic Load

Area equivalent rotor speed (rad/s)	$\bar{\omega}_1 = 314.5010$	$\bar{\omega}_2 = 313.8314$	$\bar{\omega}_3 = 314.5888$
System COI Speed (rad/s)	$\bar{\omega}_{COI}(t) = \frac{1}{M_T}\sum_{j=1}^{r} M_j\bar{\delta}_j = 314.3322$		
Area-Based TSI COI Speed (rad/s)	$\omega_1^{COI} = 0.1689$	$\omega_2^{COI} = -0.5008$	$\omega_3^{COI} = 0.2566$

Figure 12 – 15 show the plotting of TSI COI Angle, TSI COI Speed and Accelerating Power of the three areas being plotted for 15 seconds for faults at Bus 80. The graphs of Area-Based TSI: COI Angle in Figure 11 shows that the system is out of synchronism with COI Angle in each area increases to value above ±180º.

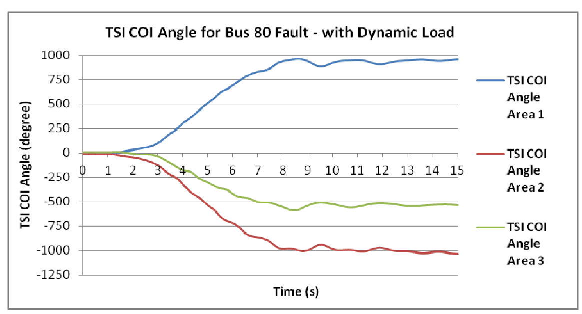

Figure 12: TSI COI Angle for Bus 80 Fault with Dynamic Load – Case2

Figure 13 illustrates the graphs for Area-Based TSI: COI Speed of each area; they oscillate at high values after disturbance occurs. Despite of reduction in magnitude later but the graph of TSI COI Speed for each area is still struggling to converge even at 15s.

Journal of Theoretical and Applied Information Technology
31st July 2013. Vol. 53 No.3

ISSN: 1992-8645 www.jatit.org E-ISSN: 1817-3195

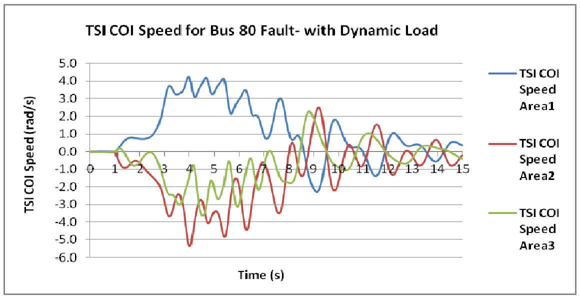

Figure 13: TSI COI Speed for Bus 80 Fault with Dynamic Load – Case2

The Accelerating Power in Figure 14 proves that the rotor angles oscillate rapidly depending on the extent of the unbalance between the mechanical input power, P_m and the electrical output power of the generator, P_e.

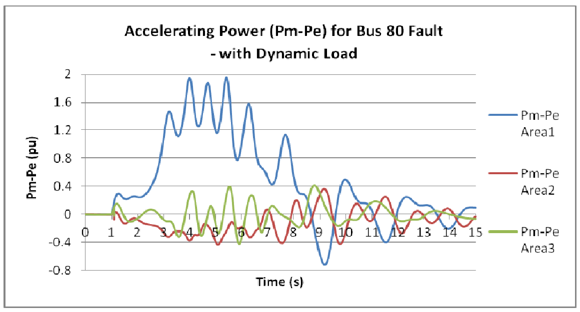

Figure 14: Accelerating Power for Bus 80 Fault with Dynamic Load – Case2

5.2 Optimization of Mechanical Input Power for IEEE 30Bus Test System using Evolutionary Computation

Simulations are carried out using TSI COI Angle and TSI COI Speed as fitness functions in the optimization algorithm of mechanical input power to synchronous generator using EP. Samples of the results are tabulated in this paper to demonstrate the consistency of the results for different number of samples and test systems.

- Case1 consists of 3 control variables of randomly different scenarios with fault clearance time of 100ms and fitness functions of:
  - Change in frequency of zero and ± 0.5Hz respectively.
  - Stability limit angle of ±180° and ±120° respectively. An angle stability limit is set at 120° in order to allow the system to have sufficient stability margin [2].
- Case 2 are meant for 3 control variables of randomly different scenarios with fault clearance time of 150ms and fitness functions of:
  - Change in frequency of zero and ± 0.5Hz respectively.
  - Stability limiting angle of ±180° and ±120° respectively.

The results for optimization process to minimize the TSI COI Angle and TSI COI Speed for 3 control variables for 20 populations are tabulated. These output data in terms of control variables are then used to calculate the TSI COI Angle and TSI COI Speed to verify the validity of the results. Case 1 provides the same set of output for each different scenario irrespective of zero change in frequency or ±0.5Hz and stability limiting angle of ±180° or ±120°. The summary of the results are tabulated in Table 5 and Table 6.

Table 5: Case 1 – Area-Based TSI COI Angle: Angle< ±180°; Frequency = 50Hz and t=100ms

Data from EP for Area 1						Area-Based TSI COI Angle for Area 1		
P_mG_1	δ_0G_1	θG_1	P_mG_2	δ_0G_2	θG_2	δ_{j1}	δ_{COI}	δ_{jCOI1}
0.6381	25.4435	21.1634	0.6205	40.6324	31.5681	33.0372	44.9456	-11.9084
0.6381	25.4435	21.1634	0.6205	40.6324	31.5681	33.0372	44.9456	-11.9084
Data from EP for Area 2						**Area-Based TSI COI Angle for Area 2**		
P_mG_3	δ_0G_3	θG_3	P_mG_4	δ_0G_4	θG_4	δ_{j2}	δ_{COI}	δ_{jCOI2}
0.5451	46.8633	11.0022	0.6625	28.0852	26.5356	37.4739	44.9456	-7.4716
0.5451	46.8633	11.0022	0.6625	28.0852	26.5356	37.4739	44.9456	-7.4716
Data from EP for Area 3						**Area-Based TSI COI Angle for Area 3**		
P_mG_5	δ_0G_5	θG_5	P_mG_6	δ_0G_6	θG_6	δ_{j3}	δ_{COI}	δ_{jCOI3}
0.5045	19.0164	20.5753	0.6638	59.5041	8.5316	39.2482	44.9456	-5.6974
0.5045	19.0164	20.5753	0.6638	59.5041	8.5316	39.2482	44.9456	-5.6974

Table 6: Case 1 – Area-Based TSI COI Speed: Angle< ±180°; Frequency = 50Hz and t=100ms

Data from EP for Area 1						Area-Based TSI COI Speed for Area 1		
P_mG_1	δ_0G_1	θG_1	P_mG_2	δ_0G_2	θG_2	ω_{j1}	ω_{COI}	ω_{jCOI1}
0.6381	25.4435	21.1634	0.6205	40.6324	31.5681	314.1675	314.1848	-0.0173
0.6381	25.4435	21.1634	0.6205	40.6324	31.5681	314.1675	314.1848	-0.0173
Data from EP for Area 2						**Area-Based TSI COI Speed for Area 2**		
P_mG_3	δ_0G_3	θG_3	P_mG_4	δ_0G_4	θG_4	ω_{j2}	ω_{COI}	ω_{jCOI2}
0.5451	46.8633	11.0022	0.6625	28.0852	26.5356	314.1801	314.1848	-0.0047
0.5451	46.8633	11.0022	0.6625	28.0852	26.5356	314.1801	314.1848	-0.0047
Data from EP for Area 3						**Area-Based TSI COI Speed for Area 3**		
P_mG_5	δ_0G_5	θG_5	P_mG_6	δ_0G_6	θG_6	ω_{j3}	ω_{COI}	ω_{jCOI3}
0.5045	19.0164	20.5753	0.6638	59.5041	8.5316	314.1948	314.1848	0.0099
0.5045	19.0164	20.5753	0.6638	59.5041	8.5316	314.1948	314.1848	0.0099

The algorithm is tested by varying the limiting angle from ±120° to ±180°and the frequency rate value to frequency range of ±0.5Hz but different fault clearance time as mention in Case 2. Table 7

ISSN: 1992-8645 www.jatit.org E-ISSN: 1817-3195

and Table 8 illustrate the results for fault clearance time of 150ms. The output of the algorithms remains to be within the acceptable range as before; however, due to the delay in the setting of fault clearance time by 50ms from Case 1, the values of TSI COI Angle and TSI COI Speed increase compared to Case 1 but still within the acceptable range.

Table 7: Area-Based TSI COI Angle; Fault Clearance Time of 150ms

Data from EP for Area 1						Area-Based TSI COI Angle for Area 1		
P_mG_1	δ_0G_1	θG_1	P_mG_2	δ_0G_2	θG_2	δ_{j1}	δ_{COI}	δ_{jCOI1}
0.6381	25.4435	21.1634	0.6205	40.6324	31.5681	33.0380	44.9520	-11.9140
0.6381	25.4435	21.1634	0.6205	40.6324	31.5681	33.0380	44.9520	-11.9140
Data from EP for Area 2						**Area-Based TSI COI Angle for Area 2**		
P_mG_3	δ_0G_3	θG_3	P_mG_4	δ_0G_4	θG_4	δ_{j2}	δ_{COI}	δ_{jCOI2}
0.5451	46.8633	11.0022	0.6625	28.0852	26.5356	37.4738	44.9520	-7.4782
0.5451	46.8633	11.0022	0.6625	28.0852	26.5356	37.4738	44.9520	-7.4782
Data from EP for Area 3						**Area-Based TSI COI Angle for Area 3**		
P_mG_5	δ_0G_5	θG_5	P_mG_6	δ_0G_6	θG_6	δ_{j3}	δ_{COI}	δ_{jCOI3}
0.5045	19.0164	20.5753	0.6638	59.5041	8.5316	39.2576	44.9520	-5.6945
0.5045	19.0164	20.5753	0.6638	59.5041	8.5316	39.2576	44.9520	-5.6945

Table 8: Area-Based TSI COI Speed; Fault Clearance Time of 150ms

Data from EP for Area 1						Area-Based TSI COI Speed for Area 1		
P_mG_1	δ_0G_1	θG_1	P_mG_2	δ_0G_2	θG_2	ω_{j1}	ω_{COI}	ω_{jCOI1}
0.6381	25.4435	21.1634	0.6205	40.6324	31.5681	314.1700	314.1925	-0.0225
0.6381	25.4435	21.1634	0.6205	40.6324	31.5681	314.1700	314.1925	-0.0225
Data from EP for Area 2						**Area-Based TSI COI Speed for Area 2**		
P_mG_3	δ_0G_3	θG_3	P_mG_4	δ_0G_4	θG_4	ω_{j2}	ω_{COI}	ω_{jCOI2}
0.5451	46.8633	11.0022	0.6625	28.0852	26.5356	314.1863	314.1925	-0.0062
0.5451	46.8633	11.0022	0.6625	28.0852	26.5356	314.1863	314.1925	-0.0062
Data from EP for Area 3						**Area-Based TSI COI Speed for Area 3**		
P_mG_5	δ_0G_5	θG_5	P_mG_6	δ_0G_6	θG_6	ω_{j3}	ω_{COI}	ω_{jCOI3}
0.5045	19.0164	20.5753	0.6638	59.5041	8.5316	314.2054	314.1925	0.0129
0.5045	19.0164	20.5753	0.6638	59.5041	8.5316	314.2054	314.1925	0.0129

If the critical clearance time needs to be longer due the performance of circuit breaker and/or the constraint of the communication system; for example, a total clearance time of 150ms based on circuit breaker clearance time of 100ms and communication time of 50ms, then the initial operating condition needs to be changed. From these findings we can deduce a conclusion that in addition to the initial operating condition of the system, fault clearance time also plays an important role in keeping the system stable.

5.3 Optimization of Mechanical Input Power for IEEE 180Bus Test System using Evolutionary Computation

The algorithm is further tested on IEEE118 Test System with 4 control variables for 20 and 40 populations. Table A1 in the Appendix tabulates the results of the algorithm for 28 generators with a limiting angle set to ±180° and 50Hz frequency; similar results are obtained for a limiting angle of ±120° and 50Hz frequency for 20 and 40 populations. It is proven that the multi-machine in IEEE118 Bus Test System is in synchronism with all the machines turning at a constant speed; the system frequency is equal to the dynamic frequency either above or below the steady state speed, ω_s [4].

6. CONCLUSIONS

This paper presents a novel contribution using Evolutionary Programming (EP) approach to optimize the mechanical input power in order to prevent transient instability in the system. The findings discovered from the experiment reveal that EP approach is able to give an optimal solution on the mechanical input power to synchronous generator and within the boundary of transient stability limit in terms of voltage, angle and frequency. While maintaining the system voltage and frequency within the acceptable limits, this approach helps to optimize the usage of fuel in generating power and also in managing the spinning reserve in power system.

REFERENCES:

[1] Hadi Saadat, *Power System Analysis.* Second Edition, New York:McGraw-Hill, 2002.

[2] Amjady, N.; Banihashemi, S.A.; *Transient Stability Prediction of Power Systems by a New Synchronism Status Index and Hybrid Classifier.* Generation, Transmission & Distribution, IET Volume: 4 Issue: 4, Page(s): 509 – 518, 2010.

[3] Kundur, P. *Introduction to the Power System Stability Problem – Basic Concept and Definitions, Mid-term and Long-Term Stability*. Power System Stability and Control: 33-34, McGraw-Hill.1994.

[4] Sauer P. W and M. A. Pai, *Power System Dynamics and Stability*. Prentice Hall, 1998.

ISSN: 1992-8645 www.jatit.org E-ISSN: 1817-3195

[5] Machowski, J.; Bialek, J W.; Bumby, JR. *Power System Dynamics Stability and Control*. 2nd Edition, John Wiley & Sons, 2008.

[6] Hayes, K.F.; Rovnyak, S.M.; Lingyan Sun; Khaliq, A.; Thyagarajan,S.; Neural networks using apparent resistance for out-of-step relaying. Power Engineering Society Winter Meeting, Volume: 1. 2002 IEEE, Page(s): 459 – 463.

[7] Paudyal, S.; Ramakrishna, G.; Sachdev, M.S.; *Application of Equal Area Criterion Conditions in the Time Domain for Out-of-Step Protection*. Volume: 25, Issue: 2. 2010, Page(s): 600-609.

[8] Billinton, R.; Kuruganty, P.R.S. *A probabilistic Index for transient Stability*. Power Apparatus and Systems, IEEE Transactions on Volume: PAS-99 , Issue: 1 1980. Page(s): 195 – 206.

[9] Abdelaziz, A.Y.; Irving, M.R.; Mansour, M.M.; El-Arabaty, A.M.; Nosseir, A.I.; *Adaptive protection strategies for detecting power system out-of-step conditions using neural networks.* Generation, Transmission and Distribution, IEE Proceedings- Volume: 145. 1998 , Page(s): 387 – 394.

[10] Chao Wang; Peng Gao; Taoxi Zhu; Wei Shao; *New method of searching for the out-of-step separation interface based on reactive power*. Transmission and Distribution Conference and Exposition, 2008. T&D. IEEE/PES. Page(s):1-5

[11] Li Li; Yutian Liu; Out-of-step splitting framework based on adaptive separation detecting criterion. Transmission & Distribution Conference & Exposition: Asia and Pacific, 2009 Page(s): 1 – 5.

[12] So, K.H. ; Heo, J.Y. ; Kim, C.H. ; Aggarwal, R.K. ; Song, K.B. ; *Out-of-step detection algorithm using frequency deviation of voltage. Generation, Transmission & Distribution, IET*. 2007 Page(s): 119-126

[13] Tang, C.K.; Graham, C.E.; El-Kady, M.; Alden, R.T.H. Transient Stability Index from Conventional Time Domain Simulation. Power Systems, IEEE Transactions on Volume: 9, Issue: 3 1994, Page(s): 1524 – 1530.

[14] A. W. Noor Izzri, A. Mohamed, *Area-Based COI-Referred Transient Stability Index for Large-Scale Power System*. International Journal of Power, Energy and Artificial Intelligence, No.1, Vol. 1. August 2008.

[15] Zulkepali, M.R.; Hashim, H.; Omar, Y.R.; Abidin, I.Z.; Yusof, S.; An Evaluation on Transient Stability of Power System using Transient Stability in Static and Dynamic Environment”APACEEE2010, CIRED.

[16] Fabozzi,D.; Van Cutsem,T. *On Angle References in Long-Term Time-Domain Simulations*. Power Systems, IEEE Transactions on Volume: PP , Issue: 99 2010 , Page(s): 1 – 2.

[17] Cheung, K.W.; *An Improved Transient Stability Index for Dynamic Security Assessment Using a Marginally Unstable Injection (MUI) Approach*. Power Engineering Society Winter Meeting, 2000. IEEE Volume: 2 2000, Page(s): 931 - 936 vol.2.

[18] Jun Qi; Guangzeng Wang; Quanyuan Jiang; Yijia Cao *Decentralized nonlinear excitation control based on wide-area measurements*. Power Systems Conference and Exposition, 2009. PSCE '09.IEEE/PES 2009, Page(s):1–5.

[19] Tangpatiphan, K.; Yokoyama, A. *Evolutionary Programming Incorporating Neural Network for Transient Stability Constrained Optimal Power Flow*. Power System Technology and IEEE Power India Conference, 2008. POWERCON 2008. Joint International Conference on 2008, Page(s): 1 – 8.

[20] Mariotto, L.; Pinheiro, H.; Cardoso, G.; Morais, A.P.; Muraro, M.R. *Power systems transient stability indices: an algorithm based on equivalent clusters of coherent generators.* Generation, Transmission & Distribution, IET Volume: 4, Issue: 11 2010, Page(s): 1223 – 1235.

[21] E. O. Schweitzer, III, D.E. Whitehead, A. Guzman, Y. Gong, and M. Donolo, *Advanced Real-Time Synchrophasor Application*. Journal of Reliable Power, 2008.

[22] PM Anderson. *Power System Protection*. McGraw-Hill. 1999.

[23] TNB Transmission Division, *Protection and Control Code of Practice (COP)*, Second Edition, September 2003.

Journal of Theoretical and Applied Information Technology
31st July 2013. Vol. 53 No.3

ISSN: **1992-8645** www.jatit.org E-ISSN: **1817-3195**

APPENDIX

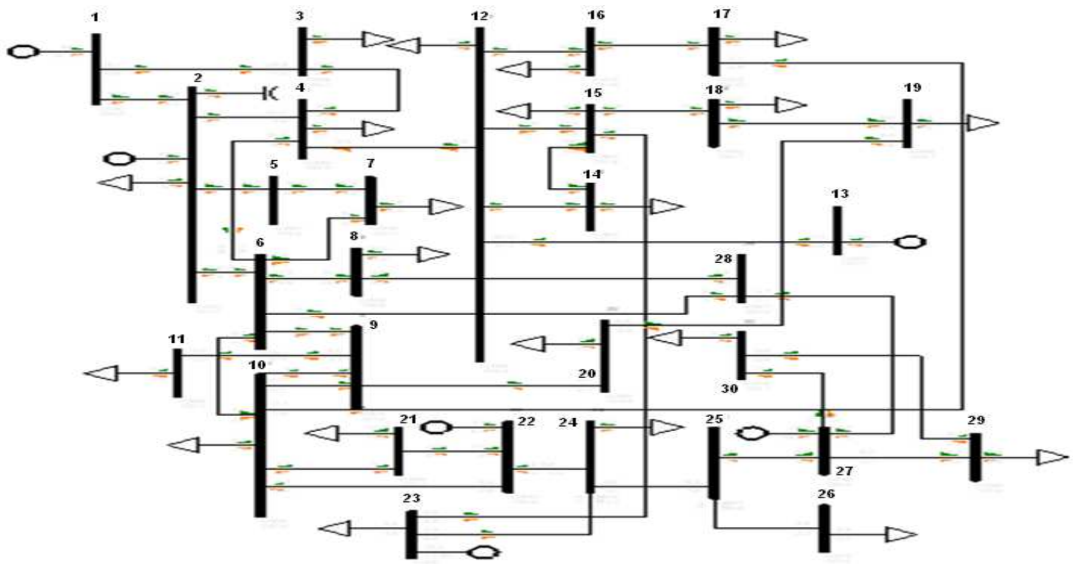

Figure A1: IEEE30 Bus Test System

Figure A2: IEEE118 Bus Test System

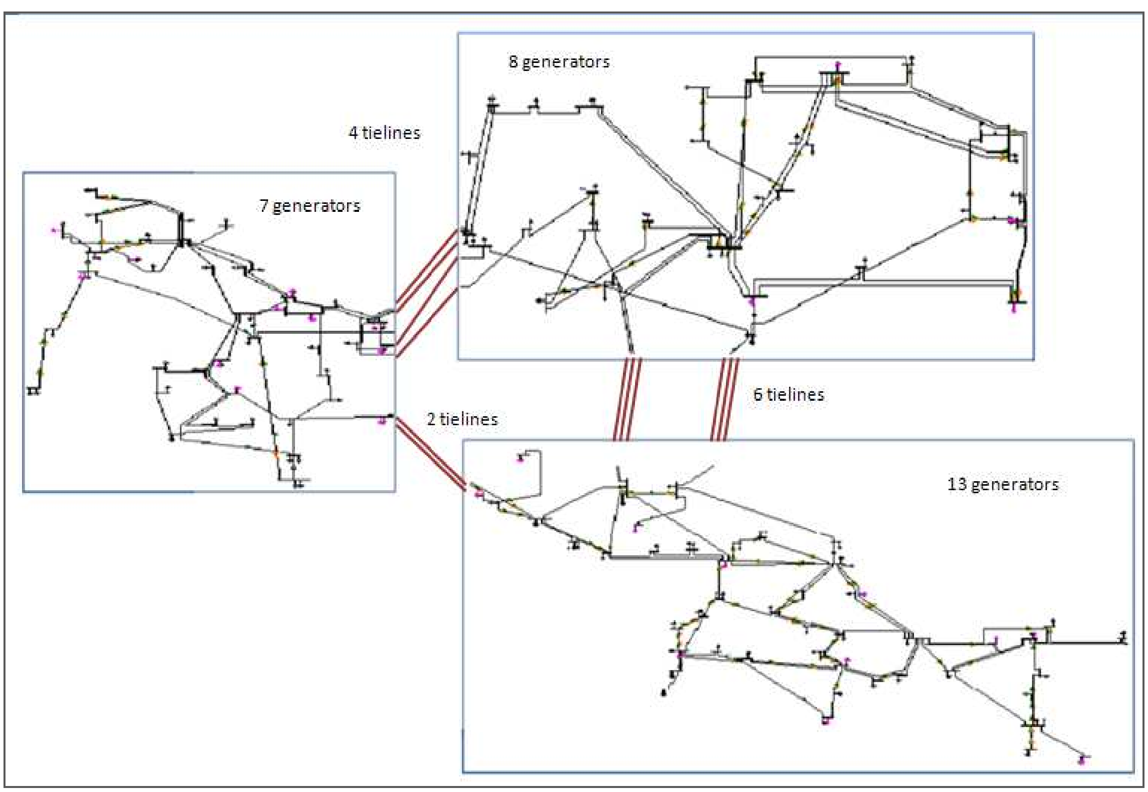

Journal of Theoretical and Applied Information Technology
31st July 2013. Vol. 53 No.3

ISSN: 1992-8645 www.jatit.org E-ISSN: 1817-3195

Table A1: Frequency Set To 50±0.5Hz And Fault Clearance Time Of 100ms For 40 Populations

	Data from EP for Area 1				Processed Data				TSI COI Angle for Area 1			TSI COI Speed for Area 1		
Gen	P_mG	δ_0G	θG	E	P_{max}	δG	ω (rad/s)	f (Hz)	δ_{j1}	δ_{COI}	δ_{jCOI1}	ω_{j1}	ω_{COI}	ω_{jCOI1}
G69	0.696	59.523	25.878	1.026	0.698	59.559	314.063	49.985						
G70	0.721	34.397	4.124	1.004	0.698	34.443	314.280	50.019						
G74	0.595	0.141	3.308	1.019	0.623	0.103	314.014	49.977						
G76	0.765	9.255	19.581	1.011	0.741	9.209	314.284	50.020						
G80	0.564	9.302	11.980	1.024	0.526	9.302	314.331	50.027						
G87	0.741	21.776	20.589	1.001	0.730	21.769	314.185	50.004	**29.348**	**25.810**	**3.538**	**314.197**	**314.181**	**0.016**
G89	0.519	47.007	18.810	1.032	0.508	46.996	314.211	50.008				f[Hz] =	f[Hz] =	
G91	0.599	40.707	7.967	1.023	0.595	40.700	314.182	50.004				50.006	50.003	
G100	0.548	53.281	22.715	1.030	0.543	53.290	314.182	50.004						
G103	0.522	46.983	5.907	1.036	0.612	46.978	314.217	50.009						
G107	0.571	34.429	6.126	1.011	0.563	34.422	314.202	50.007						
G110	0.703	15.549	10.075	1.013	0.696	15.563	314.197	50.006						
G111	0.794	9.202	21.044	1.021	0.770	9.195	314.217	50.009						
	Data from EP for Area 2				Processed Data				TSI COI Angle for Area 2			TSI COI Speed for Area 2		
Gen	P_mG	δ_0G	θG	E	P_{max}	δG	ω (rad/s)	f (Hz)	δ_{j2}	δ_{COI}	δ_{jCOI2}	ω_{j2}	ω_{COI}	ω_{jCOI2}
G40	0.579	3.013	24.987	1.039	0.578	2.564	314.165	50.001						
G42	0.695	15.550	5.757	1.011	0.692	15.549	314.178	50.003						
G46	0.477	40.708	0.772	1.032	0.465	40.697	314.188	50.005						
G49	0.645	18.998	30.753	1.037	0.644	18.998	314.162	50.000	**19.153**	**25.810**	**-6.658**	**314.174**	**314.181**	**-0.007**
G54	0.766	15.487	27.626	1.007	0.755	15.486	314.186	50.004				f[Hz] =	f[Hz] =	
G55	0.558	15.581	10.611	1.010	0.555	15.586	314.172	50.002				50.002	50.003	
G59	0.745	12.740	24.467	1.022	0.742	12.740	314.174	50.002						
G65	0.755	31.600	28.400	1.045	0.753	31.602	314.168	50.001						
	Data from EP for Area 3				Processed Data				TSI COI Angle for Area 3			TSI COI Speed for Area 3		
Gen	P_mG	δ_0G	θG	E	P_{max}	δG	ω (rad/s)	f (Hz)	δ_{j3}	δ_{COI}	δ_{jCOI3}	ω_{j3}	ω_{COI}	ω_{jCOI3}
G1	0.684	12.722	11.179	1.014	0.684	12.722	314.160	50.000						
G10	0.708	6.507	1.372	1.011	0.708	6.507	314.158	50.000						
G12	0.273	15.627	18.136	1.034	0.284	15.626	314.132	49.996	**26.034**	**25.810**	**0.223**	**314.156**	**314.181**	**-0.025**
G25	0.605	46.985	9.193	1.039	0.605	46.985	314.160	50.000				f[Hz] =	f[Hz] =	
G26	0.596	46.978	21.053	1.044	0.596	46.978	314.160	50.000				50.000	50.003	
G27	0.830	25.317	25.266	1.039	0.830	25.316	314.163	50.001						
G31	0.592	28.100	10.262	1.000	0.592	28.100	314.160	50.000						